J. Fluid Mech. (2007), *vol.* 588, *pp.* 437–462.
doi:10.1017/S0022112007007847 Printed in the United Kingdom

Diffusion of swimming model micro-organisms in a semi-dilute suspension

TAKUJI ISHIKAWA[1] AND T. J. PEDLEY[2]

[1]Department of Bioengineering and Robotics, Tohoku University, 6-6-01, Aoba, Aramaki, Aoba-ku, Sendai 980-8579, Japan

[2]Department of Applied Mathematics and Theoretical Physics, University of Cambridge, Centre for Mathematical Sciences, Wilberforce Road, Cambridge CB3 0WA, UK

(Received 12 September 2006 and in revised form 31 May 2007)

The diffusive behaviour of swimming micro-organisms should be clarified in order to obtain a better continuum model for cell suspensions. In this paper, a swimming micro-organism is modelled as a squirming sphere with prescribed tangential surface velocity, in which the centre of mass of the sphere may be displaced from the geometric centre (*bottom-heaviness*). Effects of inertia and Brownian motion are neglected, because real micro-organisms swim at very low Reynolds numbers but are too large for Brownian effects to be important. The three-dimensional movement of 64 or 27 identical squirmers in a fluid otherwise at rest, contained in a cube with periodic boundary conditions, is dynamically computed, for random initial positions and orientations. The computation utilizes a database of pairwise interactions that has been constructed by the boundary element method. In the case of *non-bottom-heavy* squirmers, both the translational and the orientational spreading of squirmers is correctly described as a diffusive process over a sufficiently long time scale, even though all the movements of the squirmers were deterministically calculated. Scaling of the results on the assumption that the squirmer trajectories are unbiased random walks is shown to capture some but not all of the main features of the results. In the case of *bottom-heavy* squirmers, the diffusive behaviour in squirmers' orientations can be described by a biased random walk model, but only when the effect of hydrodynamic interaction dominates that of the bottom-heaviness. The spreading of bottom-heavy squirmers in the horizontal directions show diffusive behaviour, and that in the vertical direction also does when the average upward velocity is subtracted. The rotational diffusivity in this case, at a volume fraction $c = 0.1$, is shown to be at least as large as that previously measured in very dilute populations of swimming algal cells (*Chlamydomonas nivalis*).

1. Introduction

The size of micro-organisms is usually much smaller than the flow field of interest, in an oceanic plankton bloom for instance, so a suspension of micro-organisms is often modelled as a continuum in which the variables are volume-averaged quantities (Pedley & Kessler 1992; Metcalfe, Pedley & Thingstad 2004). Continuum models for suspensions of swimming micro-organisms have been proposed for the analysis of phenomena such as bioconvection (e.g. Childress, Levandowsky & Spiegel 1975; Pedley & Kessler 1990; Hillesdon, Pedley & Kessler 1995; Bees & Hill, 1998; Metcalfe & Pedley, 2001). One of the most important equations in such continuum models is

the cell-conservation equation, which can be expressed as

$$\frac{Dn}{Dt} = -\nabla \cdot (n\boldsymbol{V}_c + \boldsymbol{J}_r), \tag{1.1}$$

where n is the number density of cells, $\boldsymbol{V}_c$ is the mean cell swimming velocity and $\boldsymbol{J}_r$ is the flux due to random or chaotic cell swimming. (One can add other terms, such as birth and death rates, if they are large enough to be important.) An essential ingredient of such mathematical models is a quantitative description of the random swimming behaviour of cells. Micro-organisms, even of the same species, have some genetic randomness, in size and in shape, which may induce different swimming speeds, swimming directions and swimming trajectories for each micro-organism. There may be some randomness in their reaction to light, gravity, nutrient and to other micro-organisms. In addition, the trajectories of individual cells resemble random walks (Hill & Häder 1997; Vladimirov *et al.* 2004). In the case of non-dilute suspensions of micro-organisms, the hydrodynamic interaction between cells induces frequent changes in the orientations of cells, and this interaction may also be modelled as a chaotic process. The continuum models proposed so far are, however, restricted to dilute suspensions, in which cell–cell interactions are negligible. Moreover the overall random or chaotic behaviour of swimming micro-organisms is usually described as a diffusive process, given by

$$\boldsymbol{J}_r = -\boldsymbol{D} \cdot \nabla n, \tag{1.2}$$

where $\boldsymbol{D}$ is the effective diffusivity tensor.

Childress *et al.* (1975) recognized that vertical cell swimming would lead to an aniso-tropic cell diffusivity tensor. Although they had no way of estimating the ratio of horizontal to vertical diffusivities, the results of their analysis agreed better with experiments involving *Tetrahymena* if the horizontal diffusivity were significantly less than the vertical diffusivity. Hill & Häder (1997) have plotted horizontal and vertical projections of a large number of individual trajectories of the bottom-heavy alga *Chlamydomonas nivalis*, swimming in a fluid with no imposed ambient flow so that the only orienting mechanism is gravity, which we would expect to cause the cells to swim vertically upwards on average. The cell concentrations used in the study were less than about 2×10^6 cells cm^{-3}, which corresponds to a volume fraction c of about 10^{-3}. The suspension can be regarded as dilute and the effect of interaction between micro-organisms may be supposed negligible. The observed cell trajectories show significant randomness, and the diffusive process could be correctly modelled by a biased random walk. Vladimirov *et al.* (2000, 2004) employed laser velocimetry to track a few hundred individual *C. nivalis* cells simultaneously. The results showed that cell diffusion could again be described by a random walk model. They found the rotational diffusivity D_r to be between $0.018\,\mathrm{s}^{-1}$ and $0.07\,\mathrm{s}^{-1}$, which is much smaller than the values of $0.4\,\mathrm{s}^{-1}$ to $2.2\,\mathrm{s}^{-1}$ obtained by Hill & Häder (1997). In both these experiments the cell–cell interactions were negligible, so the mechanism for the diffusive process must lie in the random differences in swimming direction and speed between cells and the intrinsic random behaviour of individual cells.

Experiments by Kessler, Hill & Häder (1992) have shown that the effect of cell-cell interactions may not be neglected at cell concentrations greater than about 5×10^6 cells cm^{-3}, in the case of *C. nivalis*, which corresponds to a volume fraction c of about 2.5×10^{-3}. The effect of cell-cell interaction on the diffusive process of micro-organisms is not clear, because previous researchers measured the diffusivity in dilute suspensions precisely in order to remove the interaction effect. Even if the

suspension is not dilute enough, diffusion is caused not only by cell-cell interactions but also by the intrinsic randomness of individual cells, so it is difficult to extract the cell-cell interaction effect from the overall results. Indeed, it may not be true that the effect of cell-cell interaction can be described by a random walk model, because, in the case of non-Brownian particles, the hydrodynamic interaction can be described deterministically by the equations of fluid dynamics. This paper will investigate whether the effect of hydrodynamic interaction between cells can be described as a diffusive process or not.

There are several kinds of diffusive phenomena, such as self-diffusion in a suspension of uniform concentration, gradient diffusion, shear-induced diffusion from regions of high shear to low (see e.g. Acrivos 1995; Wang, Murai & Acrivos 1998; Breedveld *et al.* 1998; Marchiro & Acrivos 2001; Drazer *et al.* 2002; Foss & Brady 1999, 2000; Sierou & Brady 2004). In this paper, we analyse the self-diffusion of a marked squirmer in a suspension of uniform concentration in which the only motions are those induced by the squirming (see below for a definition of squirming). Self-diffusion also appears for particles with Brownian motion. The expressions for translational and rotational diffusivities of a very dilute dispersion of independent Brownian spheres of radius a are given by

$$\boldsymbol{D}^T = \frac{kT}{6\pi\mu a}\boldsymbol{I}, \qquad \boldsymbol{D}^R = \frac{kT}{8\pi\mu a^3}\boldsymbol{I}, \tag{1.3}$$

where $\boldsymbol{D}^T$ and $\boldsymbol{D}^R$ are the translational and rotational diffusivities, respectively, k is the Boltzmann constant, T is the temperature, μ is the viscosity, and $\boldsymbol{I}$ is the unit tensor. Batchelor (1976) derived the gradient diffusivity in a dilute monodisperse system as

$$\boldsymbol{D}^T = \frac{kT}{6\pi\mu a}\boldsymbol{I}(1 + 1.45c). \tag{1.4}$$

The essential difference between Brownian spheres and squirmers is whether they show diffusivity in a very dilute suspension or not: in the absence of interaction, a squirmer swims in a straight line at constant speed, which is quite different from a diffusive process.

The model micro-organism used in this paper is exactly the same as the one used by Ishikawa, Simmonds & Pedley (2006) and Ishikawa & Pedley (2007), and will be referred to as a *squirmer*. Full details of a squirmer were given in Ishikawa *et al.* (2006), so only a brief explanation will be given here. A squirmer has a spherical shape, with surface tangential velocities given by (2.4) below. It is assumed to be neutrally buoyant, because the sedimentation velocity for typical aquatic micro-organisms is much less than the swimming speed, which can be up to hundreds of $\mu\mathrm{m\,s}^{-1}$. The centre of buoyancy of the spherical micro-organism may not coincide with its geometric centre. The model micro-organism is, therefore, force-free but may not be torque-free. The flow field around the micro-organisms is assumed to be Stokes flow and Brownian motion is not taken into account. The model of a squirmer was first proposed by Lighthill (1952), was extended by Blake (1971), and has also been used by Magar, Goto & Pedley (2003) to analyse nutrient uptake properties of a solitary squirmer.

In this paper, the three-dimensional movement of 64 or 27 identical squirmers in a fluid otherwise at rest is dynamically computed, for random initial positions and orientations, with the help of a database of pairwise interactions constructed by the boundary element method (Ishikawa *et al.* 2006). The numerical method is the same as employed by Ishikawa & Pedley (2007) and will be described only very briefly in § 2. In § 3, the diffusive behaviour of a semi-dilute suspension of *non-bottom-heavy*

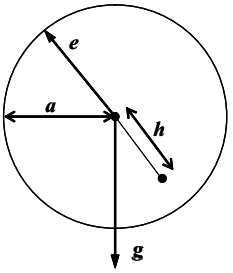

FIGURE 1. A sketch of the arrangement of a bottom-heavy squirmer. Gravity acts in the $\boldsymbol{g}$-direction, while the squirmer has orientation vector $\boldsymbol{e}$, radius a and its centre of mass is at distance h from its geometrical centre.

squirmers will be investigated. In this case, there is no preferred swimming direction. Therefore, the translational and rotational diffusivity tensors of the squirmers, if they exist, should be isotropic. The effects of volume fraction and squirming mode on the diffusive properties will be demonstrated and the scaling of the results discussed in terms of a simple random walk model. In § 4, the diffusive behaviour of a semi-dilute suspension of *bottom-heavy* squirmers will be investigated. Such squirmers tend to swim upwards on average, and the diffusivity tensor is no longer expected to be isotropic. The effects of volume fraction, squirming mode and the strength of the bottom-heaviness will be discussed.

2. Numerical methods

Only a brief outline of the numerical method will be given here; for more detail, see Ishikawa & Pedley (2007). In the absence of Brownian motion and at negligible particle Reynolds number, the equation of motion for N identical squirmers suspended in a Newtonian fluid otherwise at rest can be written as

$$-\boldsymbol{R}\cdot\boldsymbol{U} + \boldsymbol{F}_{sq} + \boldsymbol{F}_{tor} + \boldsymbol{F}_{rep} = 0. \tag{2.1}$$

Here $\boldsymbol{U}$ is a vector of dimension $6N$ containing the translational–rotational velocities of the N particles evaluated at the squirmer centre. $\boldsymbol{R}$ is the grand resistance matrix of dimension $6N \times 6N$, which is constructed by a pairwise superposition of exact results for two inert spheres, which can be found in standard texts (e.g. Kim & Karrila 1992). The pairwise additivity is an approximation, but it is expected to be justified if the particle volume fraction is not too large (defining *semi-dilute*). $\boldsymbol{F}_{sq}$ is the force–torque due to the squirming motion, which is calculated from superposition of the pairwise interactions between squirmers (Ishikawa *et al.* 2006). We should note that $\boldsymbol{F}_{sq}$ includes the effect of high multipoles, because they are captured in the computation using a boundary element method. $\boldsymbol{F}_{tor}$ represents the external torques due to the bottom-heaviness. If the distance of the centre of gravity is h from the centre of the squirmer, in the opposite direction to its swimming direction in undisturbed fluid (see figure 1), then there is an additional torque of

$$\boldsymbol{F}_{tor} = \tfrac{4}{3}\pi a^3 \rho h \boldsymbol{e} \wedge \boldsymbol{g}, \tag{2.2}$$

where ρ is the density of the cell, $\boldsymbol{e}$ is the unit orientation vector of a cell, $\boldsymbol{g}$ is the gravitational acceleration vector, and the gravitational direction is $\boldsymbol{g}/g$. $\boldsymbol{F}_{rep}$ represents the non-hydrodynamic interparticle repulsive force that is added to the system in order to avoid the prohibitively small time step needed to overcome the

problem of overlapping particles:

$$\boldsymbol{F}_{rep} = \alpha_1 \frac{\alpha_2 \exp(-\alpha_2 \varepsilon)}{1 - \exp(-\alpha_2 \varepsilon)} \frac{\boldsymbol{r}}{r}, \tag{2.3}$$

where α_1 is a dimensional coefficient, α_2 is a dimensionless coefficient and ε is the gap between squirmer surfaces non-dimensionalized by their radius. The coefficients used in this study are $\alpha_1/(\mu a U_{sol}) = 10^{-2}$ and $\alpha_2 = 10^3$, where μ is the fluid viscosity, a is the radius, and U_{sol} is the swimming speed of a solitary cell. The minimum separation obtained with these parameters is in the range 10^{-4}–10^{-5}. The effect of the repulsive force on the trajectories of cells is very small, because it acts only in the very near-field and changes the distance between particles by only around 10^{-4}. Therefore, the diffusive behaviour calculated from the trajectories of individual cells will also be unaffected by the repulsive force.

The model micro-organism used in this paper (a squirmer) is the same as the one used by Ishikawa *et al.* (2006), based on Blake (1971). The sphere's surface is assumed to move purely tangentially and these tangential motions are assumed to be axisymmetric and time-independent. Thus the tangential surface velocity on a squirmer is given as

$$\boldsymbol{u}_s = \sum_{n=1}^{2} \frac{2}{n(n+1)} B_n \left(\frac{\boldsymbol{e} \cdot \boldsymbol{r}}{r} \frac{\boldsymbol{r}}{r} - \boldsymbol{e} \right) P_n'(\boldsymbol{e} \cdot \boldsymbol{r}/r), \tag{2.4}$$

where P_n is the nth Legendre polynomial, $\boldsymbol{r}$ is the position vector and $r = |\boldsymbol{r}|$. We will follow Ishikawa *et al.* (2006), and omit squirming modes higher than the second mode, i.e. $B_n = 0$ in $\boldsymbol{u}_s$ when $n \geqslant 3$. We denote by β the ratio of second mode squirming to first mode squirming, i.e. $\beta = B_2/B_1$. The swimming speed of a solitary squirmer is $U_{sol} = 2B_1/3$, and its stresslet strength is proportional to B_2. We note that $\beta > 0$ corresponds to *pullers*, such as the bottom-heavy biflagellate algae *Chlamydomonas*, while $\beta < 0$ corresponds to *pushers*, such as spermatozoa or bacteria.

The translational cell diffusivity is a measure of the increasing displacements between pairs of particles. Thus one calculates the mean square displacement, which necessarily grows with time. If it grows more rapidly than linearly in time, then the spread is not diffusive (if proportional to t^2, it is as if the relative velocity of two spheres is constant), but if it becomes linear in time then the spread is diffusive. Thus we divide the mean square displacement by time, to see if it becomes constant: the translational cell diffusivity $\boldsymbol{D}^T$ is defined by

$$\boldsymbol{D}^T = \int_0^\infty \langle \boldsymbol{U}(t)\boldsymbol{U}(0) \rangle \, \mathrm{d}t = \lim_{t \to \infty} \frac{\langle [\boldsymbol{r}(t) - \boldsymbol{r}(0)] \, [\boldsymbol{r}(t) - \boldsymbol{r}(0)] \rangle}{2t}, \tag{2.5}$$

where $\boldsymbol{r}$ is the translational displacement. A similar calculation is carried out for angular displacement, leading to rotational cell diffusivity $\boldsymbol{D}^R$:

$$\boldsymbol{D}^R = \int_0^\infty \langle \boldsymbol{\Omega}(t)\boldsymbol{\Omega}(0) \rangle \, \mathrm{d}t = \lim_{t \to \infty} \frac{\langle [\boldsymbol{\omega}(t) - \boldsymbol{\omega}(0)] \, [\boldsymbol{\omega}(t) - \boldsymbol{\omega}(0)] \rangle}{2t}, \tag{2.6}$$

where $\boldsymbol{\omega}$ is the rotational displacement. The displacements can be calculated from the translational velocity $\boldsymbol{U}$ and the rotational velocity $\boldsymbol{\Omega}$ as follows:

$$\boldsymbol{r} = \int \boldsymbol{U} \, \mathrm{d}t, \quad \boldsymbol{\omega} = \int \boldsymbol{\Omega} \, \mathrm{d}t. \tag{2.7}$$

The brackets $\langle\rangle$ indicate an average value over M different time steps for N squirmers, so the average displacement, for example, is

$$\langle \boldsymbol{r}(t) - \boldsymbol{r}(0) \rangle = \frac{1}{MN} \sum_{m=1}^{M} \sum_{n=1}^{N} \boldsymbol{r}_n(t + m\,\mathrm{d}t) - \boldsymbol{r}_n(m\,\mathrm{d}t), \tag{2.8}$$

where $\mathrm{d}t$ is the time step used in the numerical simulation.

Bottom-heavy squirmers tend to swim upwards on average. Thus, one needs to subtract this average velocity in discussing the translational diffusivity. In such a case, $\hat{\boldsymbol{r}}$ instead of $\boldsymbol{r}$ is used in equation (2.5), where

$$\hat{\boldsymbol{r}} = \int \boldsymbol{U} - \langle \boldsymbol{U} \rangle \,\mathrm{d}t, \tag{2.9}$$

and $\langle \boldsymbol{U} \rangle$ is the average upward swimming velocity.

The effective diffusivity of a collection of particles can be specified in terms of the velocity autocorrelation function as well as in terms of the mean square displacement, as in (2.5) and (2.6). It is shown in the Appendix (equation (A 1)) that the two definitions lead asymptotically to the same answer in this case, which acts as a check on the validity of the computations.

The computational region is a cube of side L. To model a suspension of infinite extent, periodic boundary conditions are employed. A squirmer is taken to interact with the other squirmers in that periodic cell whose centre coincides with the squirmer's centre, and interactions with particles outside the cell are neglected. This treatment can be justified for $c < 0.1$. The translational displacement is calculated from (2.7), so the trajectories are traced outside the periodic cell. The time-marching is performed by the fourth-order Adams–Bashforth scheme from random initial positions and orientations. The effect of the particle number on diffusion coefficients has been checked numerically by using 27, 64 and 125 particles. Twenty-seven particles are employed for non-bottom-heavy squirmers, and 64 particles are employed for bottom-heavy ones; the difference of the diffusivities from their values for the next larger number of particles becomes about 2% or less in our parameter range. The reason why the diffusivities are not strongly dependent on the particle number is that most of the interactions are pairwise and that the effect of a third particle is very small in the semi-dilute suspension. (Batchelor & Green 1972 showed that the rheological properties of a semi-dilute suspension can be obtained just by considering two-particle interactions.) In a concentrated suspension, however, particles form clusters and the microstructure is strongly dependent on the system size, i.e. the number of particles in the computational domain. We do not discuss such high concentration cases in this study. The computation for non-bottom-heavy squirmers will be performed during the time interval of $t = 0$–1000 or more, and that for bottom-heavy squirmers will be $t = 0$–400 or more because of the high computational load when 64 particles are used. The suspension average values are calculated by averaging all particles in the computational cell from $t = 50$ to the end of the computation. It is confirmed that the probability density function for the relative position of a pair of squirmers becomes independent of specific initial conditions after $t = 50$.

All quantities are non-dimensionalized using the radius a, characteristic velocity $U_{sol} = 2B_1/3$, characteristic time a/U_{sol} and the fluid viscosity μ. There is one important dimensionless parameter in addition to β: G_{bh}. G_{bh} is the ratio of the gravitational torque to a scale for the viscous torque, assuming that U_{sol}/a is a

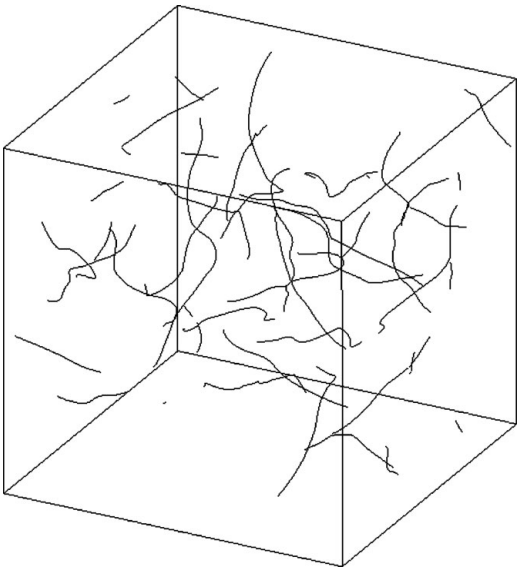

FIGURE 2. Trajectories during the five previous time intervals for 27 identical squirmers with $\beta = 5$ in a fluid otherwise at rest ($c = 0.1$).

suitable scale for the angular velocity, and is defined as

$$G_{bh} = \frac{2\pi\rho g a h}{\mu B_1}. \tag{2.10}$$

3. A semi-dilute suspension of non-bottom-heavy squirmers

3.1. *Simulation results*

In the case of non-bottom-heavy squirmers, there is no preferred orientation. If the swimming trajectories of squirmers are chaotic, the diffusivity tensor should be isotropic. Only if all squirmers start off squirming in exactly the same direction, on the other hand, do they remain so, and the spreading process is no longer diffusive. Here, we will mainly discuss the average of the three diagonal components in the diffusion tensors defined as

$$D^T = \frac{D^T_{xx} + D^T_{yy} + D^T_{zz}}{3}, \quad D^R = \frac{D^R_{xx} + D^R_{yy} + D^R_{zz}}{3}. \tag{3.1}$$

The three-dimensional movement of 27 identical non-bottom-heavy squirmers with $\beta = 5$ in a fluid otherwise at rest is computed with volume fraction $c = 0.1$. The instantaneous positions of the squirmers and their trajectories over the five previous time intervals are shown in figure 2. Note, however, that trajectories for calculating the translational displacement are traced outside the periodic cell. We see that the trajectories of squirmers are not straight, because the hydrodynamic interaction between squirmers causes them to change direction. The results for two-squirmer interactions with $\beta > 0$ have shown that the squirmers first attract each other, then they change their orientation dramatically when they are in near-contact, and finally they separate from each other (see Ishikawa *et al.* 2006).

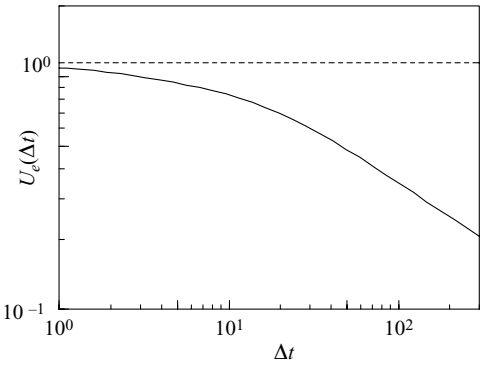

FIGURE 3. Effective velocity of squirmers with $\beta = 5$ ($c = 0.1$). The broken line represents the value of $U_e(0)$.

Before discussing the diffusivities, we first introduce an effective velocity $U_e(\Delta t)$ defined as

$$U_e(\Delta t) = \left\langle \left| \frac{\boldsymbol{r}(t+\Delta t) - \boldsymbol{r}(t)}{\Delta t} \right| \right\rangle. \tag{3.2}$$

This effective velocity with $\beta = 5$ and $c = 0.1$ is shown as a function of Δt in figure 3, in which the broken line represents the value of $U_e(0)$. We see that U_e decreases with increasing Δt and the value of $U_e(0)$ is greater than one. If there were no interaction between squirmers, the swimming velocities of all the squirmers should be one. The decrease of $U_e(\Delta t)$ with increasing Δt indicates that there are interactions between squirmers, causing repeated changes in swimming directions. However, the value of $U_e(0)$ in this case is about 1.14, which means the absolute value of the instantaneous velocity is increased by the interaction, because a given squirmer is always swimming in the flow field generated by others. This effect can be shown analytically when the squirmers are far enough apart for a far-field description of the velocity field to be justified, as follows. Let a solitary squirmer be at the origin of coordinates with the orientation vector $\boldsymbol{e}$. The velocity field generated by the squirmer is given by:

$$\begin{aligned} \boldsymbol{u}(\boldsymbol{r}) = &-\frac{1}{3r^3} B_1 \boldsymbol{e} + \frac{2}{3r^3} B_1 \frac{\boldsymbol{e}\cdot\boldsymbol{r}}{r}\frac{\boldsymbol{r}}{r} + \left(\frac{1}{r^4} - \frac{1}{r^2}\right) B_2 P_2 \frac{\boldsymbol{r}}{r} \\ &+ \frac{1}{3r^4} B_2 P_2' \left(\frac{\boldsymbol{e}\cdot\boldsymbol{r}}{r}\frac{\boldsymbol{r}}{r} - \mathrm{e} \right) \end{aligned} \tag{3.3}$$

(see Ishikawa *et al.* 2006). Let an additional squirmer be introduced at $\boldsymbol{r}_2$ with the orientation vector $\boldsymbol{e}_2$. If the two squirmers' separation is great enough, i.e. $|\boldsymbol{r}_2| \gg 1$, the velocity of the second squirmer can be approximated by the sum of two velocities: (i) the velocity of a solitary squirmer at $\boldsymbol{r}_2$ with orientation $\boldsymbol{e}_2$, and (ii) the velocity generated at $\boldsymbol{r}_2$ by the first squirmer in the absence of the second squirmer, which is given by (3.3). If one assumes an isotropic probability distribution for two squirmers' relative position and orientation, which may be true if they are far apart, the following inequality is satisfied:

$$\begin{aligned} |\boldsymbol{U}_2(r)| &= \frac{1}{4\pi r^2} \iiint_{r=\mathrm{const}} |\boldsymbol{U}_2(\boldsymbol{e}, \boldsymbol{e}_2, \boldsymbol{r}_2)| \mathrm{d}\boldsymbol{e}\, \mathrm{d}\boldsymbol{e}_2\, \mathrm{d}\boldsymbol{r}_2 \\ &= \int_0^\pi \int_0^\pi \frac{\sin\theta \sin\phi}{4} \sqrt{(1 + |\boldsymbol{u}(\boldsymbol{r}_2)| \cos\phi)^2 + (|\boldsymbol{u}(\boldsymbol{r}_2)| \sin\phi)^2}\, \mathrm{d}\phi\, \mathrm{d}\theta \geqslant 1, \end{aligned} \tag{3.4}$$

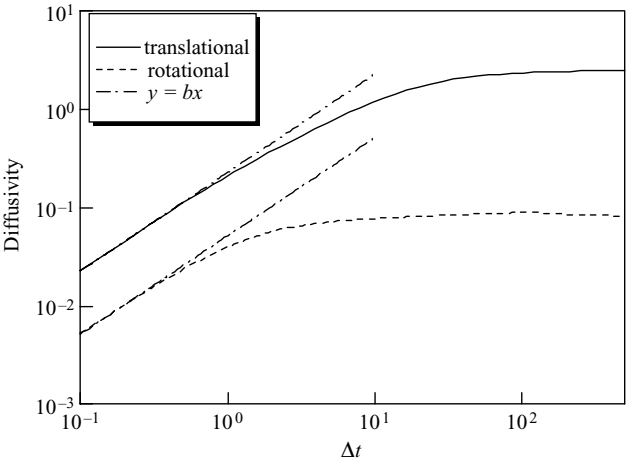

FIGURE 4. Translational and rotational diffusivities of squirmers during the time interval of Δt ($\beta = 5$ and $c = 0.1$).

where θ is the angle between $\boldsymbol{e}$ and $\boldsymbol{r}_2$, and ϕ is the angle between $\boldsymbol{e}_2$ and $\boldsymbol{u}(\boldsymbol{r}_2)$. This inequality indicates that the absolute value of the instantaneous velocity is increased by the interaction, at least in the far-field.

We have also performed some trial simulations of a rather dense suspension, with $c = 0.3$ for example, although the approximation of pairwise additivity may not be accurate then. The results show that the effective velocity is much less than one if c is large enough, even at $\Delta t = 0$, because there is not enough room for squirmers to swim freely.

The instantaneous translational–rotational velocities are integrated in time, as given by (2.7), and translational–rotational effective diffusivities are calculated from (3.1) as

$$\frac{\langle |\boldsymbol{r}(t+\Delta t) - \boldsymbol{r}(t)|^2 \rangle}{2\Delta t}, \quad \frac{\langle |\boldsymbol{\omega}(t+\Delta t) - \boldsymbol{\omega}(t)|^2 \rangle}{2\Delta t}. \tag{3.5}$$

The results with $\beta = 5$ and $c = 0.1$ are shown in figure 4 on a log-log plot. For comparison, lines of slope 1 are drawn as well. If there were no interaction between squirmers, the translational velocity of the squirmers would be constant, and the effective diffusivity would be proportional to Δt. We see from figure 4 that the inclination is about one when $\Delta t < 2$, which means that most of the squirmers swim constantly in their original directions over a short time interval. When $\Delta t > 2$, on the other hand, the inclination decreases from one, reflecting the occurrence of the hydrodynamic interactions.

Similarly, if there were no interaction between squirmers, the rotational velocity of the squirmers should be zero. Rotational square displacements appear because of the interactions, and the effective rotational diffusivity varies approximately linearly with Δt when $\Delta t < 1$. This result indicates that the squirmers rotate with almost constant angular velocities when $\Delta t < 1$. Over a short time interval, the configuration of squirmers in a computational cell does not change significantly, and the rotational velocities caused by the interactions between squirmers are similar. Over a long time interval, however, the configuration changes considerably, and the rotational velocities also change as time goes by. Thus the inclination of the slope of the rotational diffusivity curve in figure 4 becomes less than one when $\Delta t > 1$.

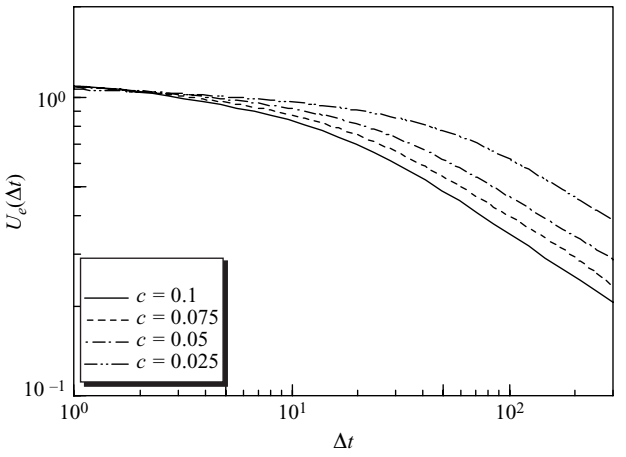

FIGURE 5. Effect of volume fraction on the effective velocity of squirmers with $\beta = 5$. (*a*) Translational diffusivity, (*b*) rotational diffusivity.

We note that both translational and rotational diffusivities converge to constant values if Δt is taken long enough. Therefore, the spreading of squirmers is correctly described as a diffusive process over a sufficiently long time scale, even though all the movements of the individual squirmers were deterministic. The diffusivity is larger for translation than for rotation, because a solitary squirmer swims with a constant translational velocity but without a rotational velocity. The time interval for constant diffusivity to appear is longer for translation than for rotation. In § 3.2 we develop a scaling argument to attempt to explain this.

The effect of volume fraction has been investigated, and the results for the effective velocity at different values of c are shown in figure 5 ($\beta = 5$). We see that U_e decreases more rapidly with Δt for larger values of c. This is because the interaction between squirmers increases with c, with more frequent changes in direction. The absolute value of the instantaneous velocity, $U_e(0)$, increases slightly with c in this range, though this is not distinguishable in figure 5. This is because the hydrodynamic interaction tends to increase the instantaneous velocity, in the semi-dilute regime, as mentioned above.

The effect of volume fraction on the translational and rotational diffusivities is shown in figures 6(*a*) and 6(*b*), respectively ($\beta = 5$). It is found that the translational diffusivity decreases with increasing c, because more frequent direction changes prevent the squirmers from spreading so fast. The rotational diffusivity on the other hand increases with increasing c, again because of the more frequent direction changes.

The parameter β is the ratio of second-mode squirming to first-mode squirming in (2.4), i.e. $\beta = B_2/B_1$. The values of β used here are from -5 to 10; the velocity fields generated by a solitary squirmer with $\beta = 1$ and 5 can be found in Ishikawa *et al.* (2006); in particular, when $\beta > 1$, there is a recirculation region behind the squirmer, and when $\beta < -1$ there is one in front. The values $|\beta| = 5$ and 10 are chosen in order to observe in an obvious way the effect of second-mode squirming. The effect of β on the effective velocity is shown in figure 7 ($c = 0.1$). We see that the effective velocity decreases more rapidly as $|\beta|$ increases. This is because the interactions between squirmers increase with $|\beta|$ (see Ishikawa *et al.* 2006), and the interactions cause changes in swimming direction. The absolute value of instantaneous velocity, $U_e(0)$, increases slightly with β when $\beta > 0$, because the hydrodynamic interaction

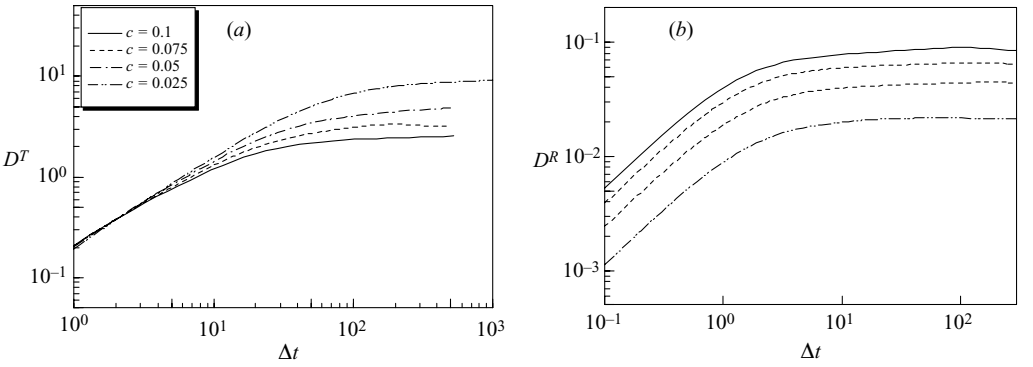

FIGURE 6. Effect of volume fraction on the diffusivities of squirmers during the time interval of Δt ($\beta = 5$).

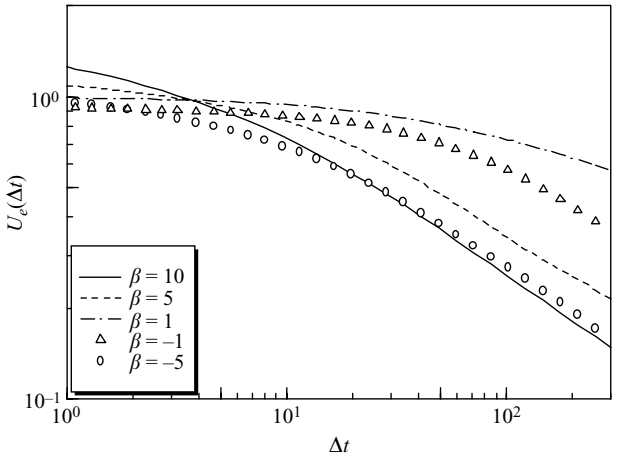

FIGURE 7. Effect of β on the effective velocity of squirmers ($c = 0.1$). (*a*) Translational diffusivity, (*b*) rotational diffusivity.

has the effect of increasing the velocity, in the semi-dilute regime, as discussed before. However, when $\beta = -1$, $U_e(0)$ is less than one because the effective repulsion between squirmers with $\beta = -1$ tends to reduce the velocity of one squirmer relative to another. Also the rate of reduction of $U_e(\Delta t)$ with Δt is greater for negative β than for positive β of the same magnitude. In general terms, though, the effect of increasing $|\beta|$ is similar to that of increasing c, because both increase the rate of hydrodynamic interactions.

The effect of β on the translational and rotational diffusivities is shown in figures 8(*a*) and 8(*b*), respectively ($c = 0.1$). The translational spreading for $\Delta t < 1$ is increased as $|\beta|$ is increased (especially for $\beta > 0$ because this increases the instantaneous velocity of squirmers). The translational diffusivity for $\Delta t > 20$, on the other hand, is decreased by $|\beta|$ because of the increased interaction between squirmers. The time interval for squirmers to show an approximately constant translational diffusivity increases as $|\beta|$ decreases, and diffusive spreading was not found for $\beta = +1$, even for Δt as large as 300.

The rotational diffusivity always increases with increasing $|\beta|$, because the rotational velocity is generated by the interaction and the interaction increases with increasing

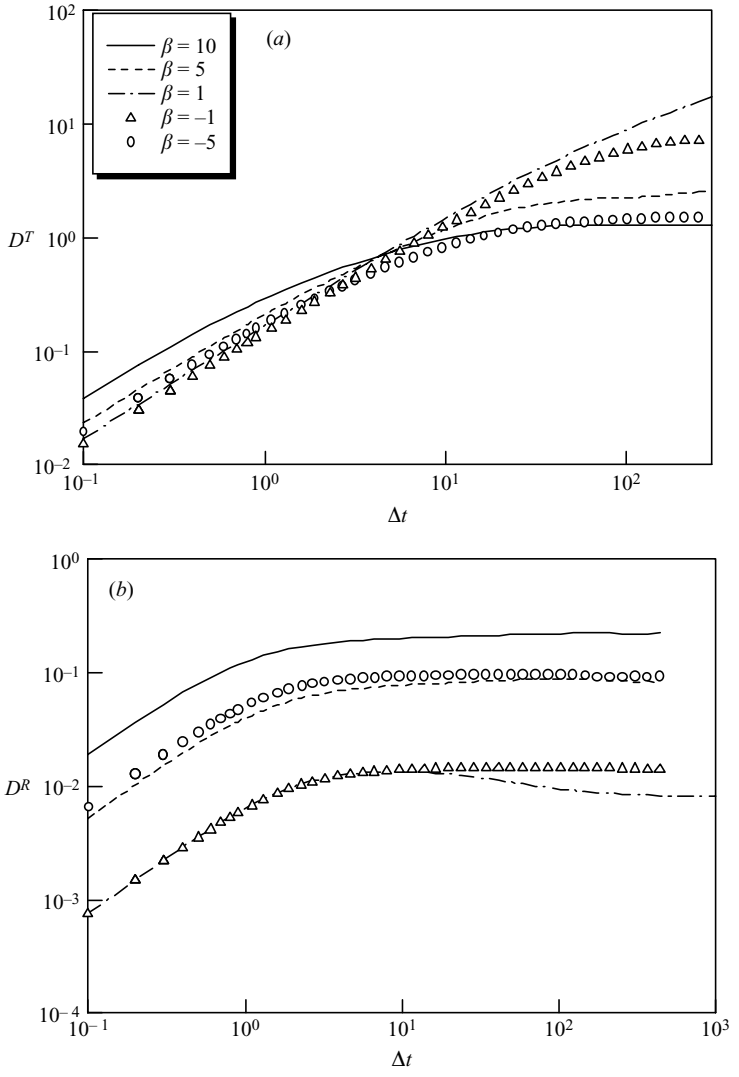

FIGURE 8. Effect of β on the diffusivities of squirmers during the time interval of Δt ($c = 0.1$). (*a*) Translational diffusivity, (*b*) rotational diffusivity.

$|\beta|$. The time interval for squirmers to show rotational diffusivity is also much less affected by β than for translational diffusivity. We currently have no explanation for the reduction in D^R for $10 < \Delta t < 100$ in the case $\beta = +1$.

3.2. *Scaling*

In the absence of interactions the translational velocity of a squirmer is a constant, $U_{sol}\boldsymbol{e}$, and its rotational velocity is zero. Interactions with neighbours mean that a squirmer rotates, and its translational velocity changes primarily because of the change of $\boldsymbol{e}$. Neither the rotational velocity nor the translational velocity will change significantly unless squirmers experience a near collision. Thus the motion might be expected to resemble a random walk of runs interspersed with near collisions.

The length scale between near collisions will be the effective mean free path, ℓ_{mfp}. If we assume that squirmers swim with a constant speed U_{sol} between collisions, then the typical time between collisions will be $t_{mfp} = \ell_{mfp}/U_{sol}$. Also the volume swept out by a squirmer in time t will be around $V_p = \pi a^2 U_{sol} t_{mfp}$, where it is assumed that anything within a cylinder of radius a will be encountered. Thus the number of particles within V_p is $nV_p = 3cU_{sol}t_{mfp}/(4a)$; if this number is assumed to be unity, we have that, in dimensionless terms,

$$t_{mfp} = \frac{4}{3c}. \tag{3.6}$$

For $c = 0.1$ this time is about 13.3. We see in figure 4 that the time interval needed before the translational diffusivity becomes constant is larger than this value, because the motion of squirmers does not become chaotic until several collisions have taken place.

On the other hand, the time required for a significant change of orientation will be the effective duration of a *collision*, rather than the elapsed time between collisions. This will be independent of the number of collisions as long as there are not so many of them that the squirmers are continuously colliding. Thus the time after which the rotational diffusivity becomes constant should be independent of cell concentration c as long as c is not too large. The validity of these time-scales can be checked by replotting the results of figure 6. In figure 9(*a*) we plot D^T divided by its large-time value, D^T_{inf}, against $\Delta t/t_{mfp}$. The curves collapse completely, indicating that the time-scale should be scaled in proportion to c^{-1}, as in (3.6). Figure 9(*b*) shows that the D^R/D^R_{inf} curves do not collapse when time is scaled in this way, whereas figure 9(*c*) shows that these curves do collapse when time is not rescaled.

It is also possible to propose scalings with c for the magnitudes of the effective diffusivities, $D^{T,R}_{inf}$. In the case of translational spreading, the random walk model suggests that $D^T_{inf} = (1/3)U_{sol}\ell_{mfp}$ or, in dimensionless terms,

$$D^T_{inf} = \frac{1}{3}t_{mfp} = \frac{4}{9c}. \tag{3.7}$$

For $c = 0.1$, this is about 4.4, which is somewhat larger than the value seen in figure 4, but the principal prediction is that D^T_{inf} is inversely proportional to c. In the dilute limit, i.e. $c \to 0$, a squirmer swims with a constant velocity, and the square displacement is proportional to the square time interval. Thus, the translational diffusivity diverges when $c \to 0$, which means that the spreading of squirmers is no longer diffusive. This is because the orientational change in squirmers is caused by hydrodynamic interactions in this study. In the rotational case, a similar random walk model implies that

$$D^R_{inf} = \frac{\langle \Delta\omega^2 \rangle}{6t_{mfp}}, \tag{3.8}$$

where $\langle \Delta\omega^2 \rangle$ is the mean square angular displacement during one (near-) collision. This latter quantity should not depend on the distance travelled between collisions and therefore should be independent of c. Thus (3.8) predicts that $D^R_{inf} \propto (t_{mfp})^{-1} \propto c$.

To test these predictions we plot D^T_{inf} and D^R_{inf} against c (on a log-log plot) in figure 10(*a*) and 10(*b*). The straight lines in the figure have slope ± 1; the graphs thus show that both the above predictions are borne out by the computed results.

However, in this discussion we have not considered the value of β; the results used for figures 9 and 10 were all for $\beta = 5$. When $\beta = 1$, on the other hand, the simulations show that squirmers sometimes do not change their swimming velocities

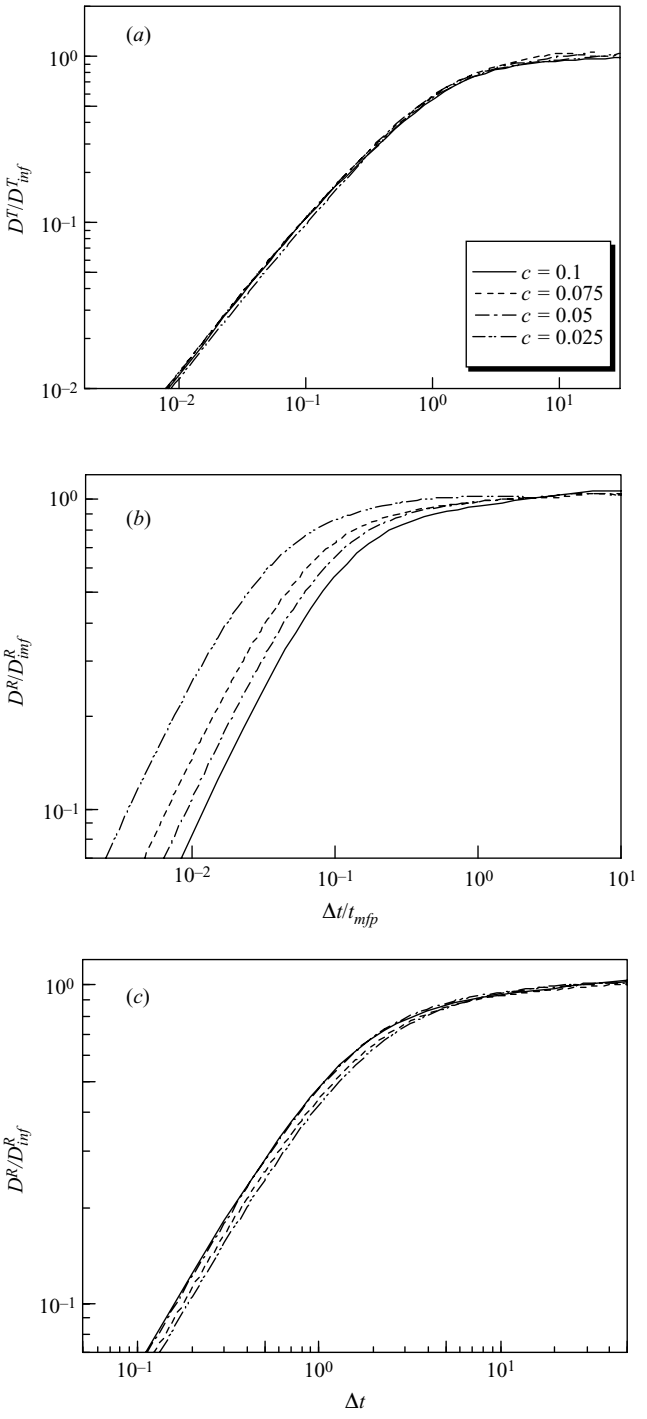

FIGURE 9. The results of figure 6 are replotted by using different characteristic time t_{mfp} or unscaled Δt, in which the vertical axis is normalized by D_{inf}. (*a*) Translational diffusivity replotted against $\Delta t/t_{mfp}$, (*b*) rotational diffusivity replotted against $\Delta t/t_{mfp}$, (*c*) rotational diffusivity, Δt is unscaled.

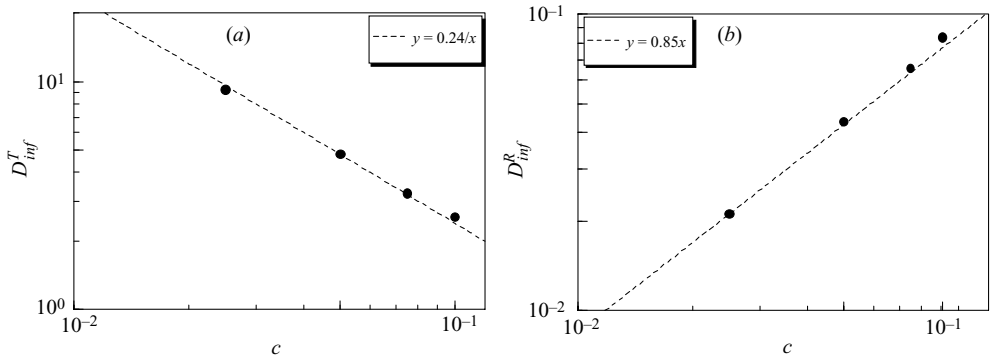

FIGURE 10. Correlation between D_{inf} and c ($\beta = 5$). D_{inf} is the converged diffusivity after a sufficiently long time.

significantly for long periods of time; it is only *very* near collisions that give rise to dramatic changes of direction. The larger $|\beta|$ is the greater the cell separation at which significant interactions occur, and the stronger the interactions at a given separation. Thus both D^T_{inf} and D^R_{inf} increase with $|\beta|$, while the time for D^T to become approximately constant increases as $|\beta|$ decreases (figure 8). We do not have an analytical prediction for these variations with β.

4. A semi-dilute suspension of bottom-heavy squirmers

If squirmers are bottom-heavy, external gravitational torques are generated when they are not oriented vertically, and they tend to swim upwards on average. The gravitational direction is taken in the $-\boldsymbol{y}$-direction in this study. G_{bh} is the ratio of the gravitational torque to a scale for the viscous torque based on the squirming velocity, as defined by (2.10). If one assumes that the micro-organisms swim in water at 10 body lengths per second with their centre of mass $0.2a$ down from the geometric centre, G_{bh} is about 5 for micro-organisms with radius of 12.5 μm, and about 50 for micro-organisms with radius of 125 μm. The parameter range used in this section is $G_{bh} = 0 - 100$. The only examples of bottom-heavy micro-organisms known to us are biflagellate algae, such as *Chlamydomonas* and *Dunaliella*, which are pullers and hence modelled by $\beta > 0$; therefore there will be little attention paid to the $\beta < 0$ case in this section.

The three-dimensional movement of $N = 64$ identical bottom-heavy squirmers with $G_{bh} = 10$ and 100 in a fluid otherwise at rest is computed, the standard case having $\beta = 5$ and $c = 0.1$. The instantaneous positions of squirmers and their trajectories over five time intervals are shown in figure 11 for the $G_{bh} = 100$ case (cf. figure 2). We see that the bottom-heavy squirmers basically swim upwards, but do not swim in straight lines. The interactions between squirmers generate translational and rotational velocities, which asymptotically increase as $\log \varepsilon^{-1}$, where ε is the dimensionless minimum separation between squirmer surfaces, in the near-field (see Ishikawa *et al.* 2006). Therefore, the hydrodynamic interaction can generate large translational and rotational velocities when ε is small enough, even though the gravitational effect is strong. The trajectories of two bottom-heavy squirmers with vertical initial orientations have been shown in Ishikawa *et al.* (2006). The results (for $\beta > 0$) show that the squirmers attract each other at first, then they swim together with similar orientations at small angles to the vertical, and finally they separate from each other.

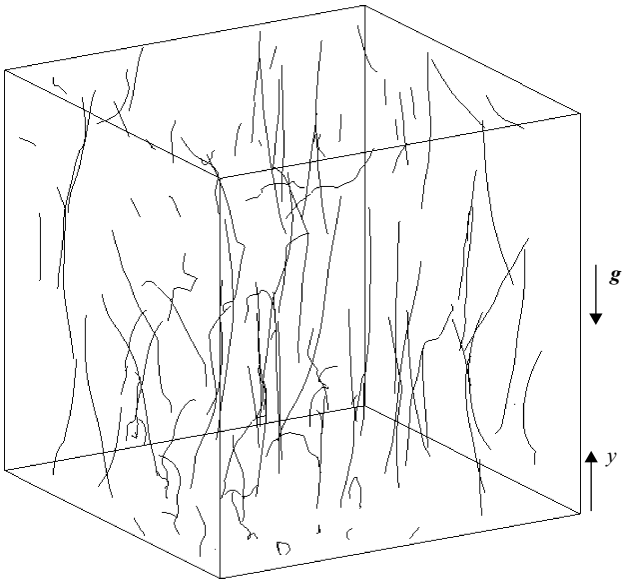

FIGURE 11. Trajectories during the five previous time intervals for 64 identical bottom-heavy squirmers with $G_{bh} = 100$ and $\beta = 5$ in a fluid otherwise at rest ($c = 0.1$). Gravitational direction is taken to be $-\boldsymbol{y}$.

As in Ishikawa & Pedley (2007), we introduce a normalized angular probability density function, defined as

$$p'(\theta) = \frac{2}{nV\sin(\theta)} \int\int_{\theta=\text{const}} P(\boldsymbol{r}, \boldsymbol{e})\, \mathrm{d}A_e\, \mathrm{d}V, \tag{4.1}$$

where $P(\boldsymbol{r}, \boldsymbol{e})$ is the probability that there is a squirmer centred at $\boldsymbol{r}$ with orientation vector $\boldsymbol{e}$ within the solid angle $\mathrm{d}A_e$, and θ is the angle from the y-axis. $P(\boldsymbol{r}, \boldsymbol{e})$ satisfies the following equation:

$$\int\int P(\boldsymbol{r}, \boldsymbol{e})\, \mathrm{d}A_e\, \mathrm{d}V = N. \tag{4.2}$$

If one assumes isotropic orientation of squirmers, then $p'(\theta) = 1$ for all θ. If one assumes that the intrinsic tendency for the cells to change direction chaotically is independent of the instantaneous direction, this process is analogous to that of colloidal particles in suspension under the action of rotary Brownian motion. Brenner & Weissman (1972) derived $p'(\theta)$ for dipolar spherical particles with rotational Brownian motions, and the solution of the Fokker–Planck equation is given by the Fisher distribution as:

$$p'(\theta) = \frac{\lambda}{\sinh\lambda} \exp(\lambda\cos(\theta)), \tag{4.3}$$

where λ is a coefficient that represents the intensity of the randomizing process. In our case, however, the intrinsic tendency for the squirmers to change direction depends on the configuration of surrounding squirmers, so equation (4.3) based on rotational Brownian motion may not be applicable.

The results for $p'(\theta)$ at various values of G_{bh} are shown in figure 12. When $G_{bh} = 0$ the $p'(\theta)$ distribution should be isotropic, and $p'(\theta) \approx 1$ for any θ. When $G_{bh} = 10$ the

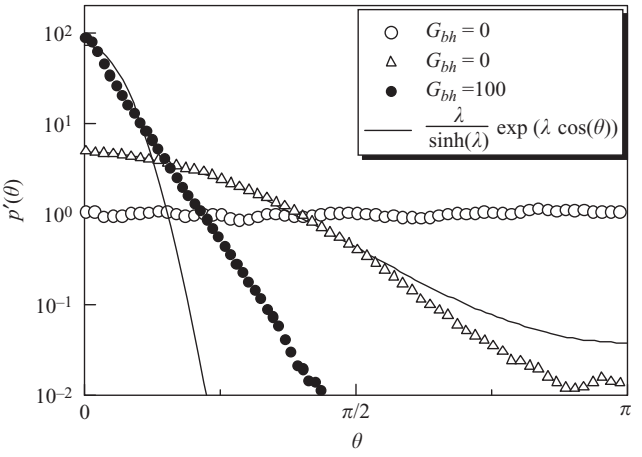

FIGURE 12. Normalized probability density function distribution for $G_{bh}=$ 0, 10 and 100 under the condition of $\beta=5$ and $c=0.1$. The function is fitted by the method of least squares. (*a*) Normal definition of the effective velocity, (*b*) effective upward swimming velocity.

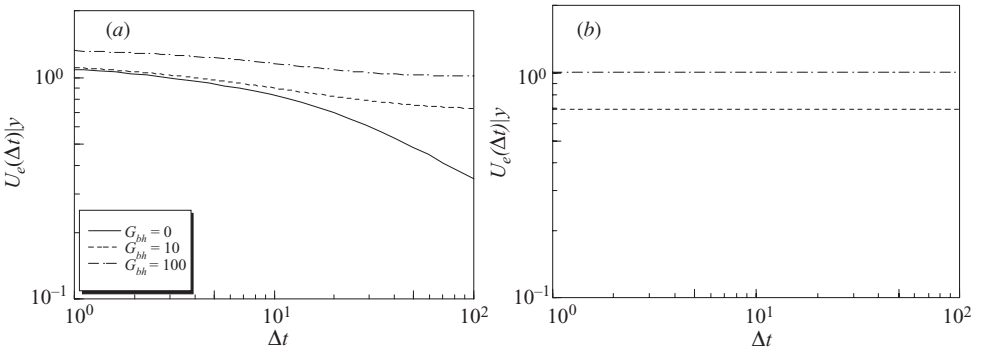

FIGURE 13. Effect of G_{bh} on the effective velocity of bottom-heavy squirmers ($\beta=5$ and $c=0.1$). (*a*) xx-component, (*b*) yy-component.

$p'(\theta)$ distribution has a peak at $\theta=0$, because the bottom-heavy squirmers tend to orientate toward the y-direction. An effective value of λ in the function given by (4.3) is obtained from a least-squares fit ($\lambda=2.43$, 38.6 for $G_{bh}=10$, 100, respectively), and the function is shown in the figure as well. It is found that the results for $G_{bh}=10$ shows good agreement with equation (4.3); it follows that the effect of interactions between squirmers can be quite accurately modelled as a biased random walk in this case. However, when $G_{bh}=100$ the $p'(\theta)$ distribution has a large peak at $\theta=0$, and squirmers cannot rotate as far as π radians. The fit to equation (4.3) is much worse in this case, as shown in figure 12. When $G_{bh}=100$ the strong gravitational torque restricts the squirmer's rotational motion, and many squirmers have similar orientations.

The effective velocity defined by (3.2) is shown in figure 13(*a*) ($\beta=5$ and $c=0.1$). If squirmers are bottom-heavy, the effective velocity does not tend to zero even when Δt becomes very large. This is because the squirmers tend to swim upwards again after every interaction, as shown in figure 11. The effective upward swimming velocity

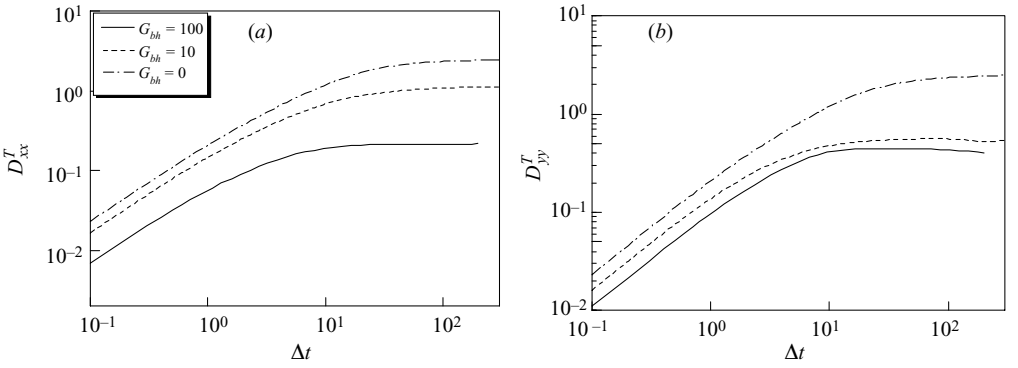

FIGURE 14. Effect of G_{bh} on the translational diffusivity of bottom-heavy squirmers during the time interval of Δt ($\beta = 5$ and $c = 0.1$). (*a*) xx-component, (*b*) yy-component.

can be defined as

$$U_e(\Delta t)|_y = \left\langle \left| \frac{r_y(t + \Delta t) - r_y(t)}{\Delta t} \right| \right\rangle, \tag{4.4}$$

and the result for this quantity is shown in figure 13(*b*). We see that the effective upward swimming velocity changes little with Δt, and that it increases with increasing G_{bh}.

In the case of bottom-heavy squirmers the diffusivity tensor (when it exists) is no longer isotropic. The gravitational direction is taken in the $-y$-direction and we will discuss separately the xx- and yy-components of the diffusivity tensor. (The zz-component should be the same as the xx-component.) The results for the translational diffusivity at $G_{bh} = 0$, 10 and 100 are shown in figures 14(*a*) and 14(*b*) ($\beta = 5$ and $c = 0.1$). When $G_{bh} = 10$ or 100, the xx-component converges to a constant value if Δt is long enough. Therefore, the horizontal spreading of bottom-heavy squirmers can be correctly described as a diffusive process over a sufficiently long time scale. The xx-component decreases with increasing G_{bh}, because the orientations of bottom-heavy squirmers are concentrated around the y-axis and movement in the x-direction is suppressed. D^T_{yy} also shows a tendency similar to D^T_{xx}. Thus, we can say that the vertical spreading of bottom-heavy squirmers, relative to their average upward velocity, can also be described as a diffusive process over a sufficiently long time scale.

The results for the rotational diffusivity tensor for $G_{bh} = 0$, 10 and 100 are shown in figures 15(*a*) and 15(*b*) ($\beta = 5$ and $c = 0.1$). The gravitational direction is taken in the $-y$-direction, so rotation in the x- or z-direction is suppressed by the torque due to bottom-heaviness. We see that the xx component of the rotational diffusivity converges to a constant value even when the gravitational effect is very large; therefore the rotation of bottom-heavy squirmers about a horizontal axis can be described as a diffusive process over a sufficiently long time scale. The xx-components have similar values when $G_{bh} = 0$ and 10, though the $G_{bh} = 100$ case shows a much lower value. This is because the hydrodynamic interaction dominates the bottom-heaviness even for $G_{bh} = 10$, and squirmers with $G_{bh} = 0$ and 10 can rotate through π radians (see figure 12). In the case of $G_{bh} = 100$, however, squirmers cannot rotate through π radians, and the rotational motion is strongly restricted by gravity. The yy-component shows a similar tendency to the xx-component, though the effect of G_{bh} is smaller. The torque due to the bottom-heaviness does not have a y-component, so the bottom-heaviness has less effect on the yy-component than on the xx-component. The rotation

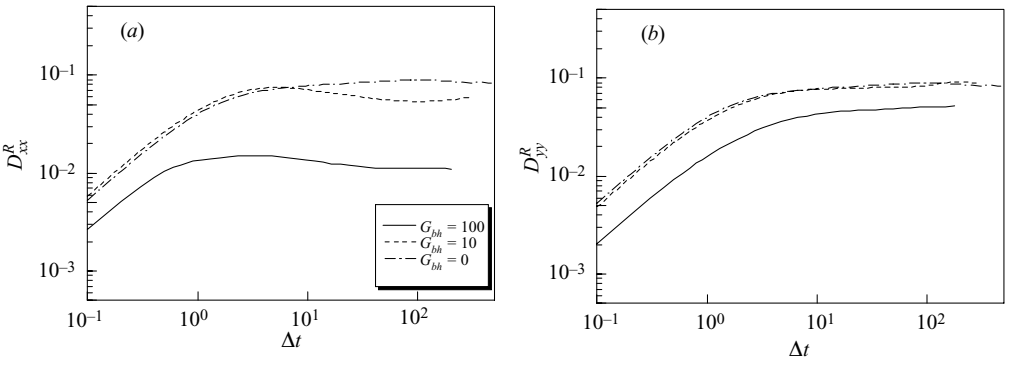

FIGURE 15. Effect of G_{bh} on the rotational diffusivity of bottom-heavy squirmers during the time interval of Δt ($\beta = 5$ and $c = 0.1$). (*a*) Comparison with various c-conditions, (*b*) comparison with the function fitted by the method of least squares.

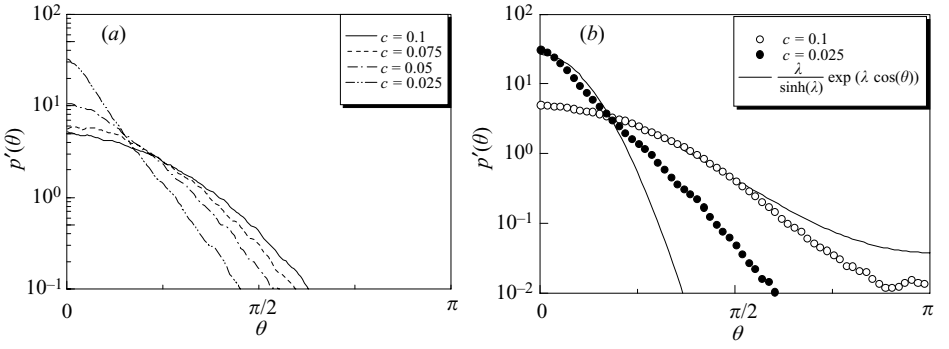

FIGURE 16. Effect of volume fraction on the normalized probability density function distribution ($G_{bh} = 10$ and $\beta = 5$).

of bottom-heavy squirmers in all directions shows diffusive behaviour, though the $p'(\theta)$ distribution for $G_{bh} = 100$ in figure 12 does not correspond to the random walk equation (4.3) for any value of λ. Actually the tendency for squirmers to change direction depends on the instantaneous configuration of surrounding squirmers, and all the movements of the individual squirmers are deterministically calculated. The hydrodynamic interaction is not a random process, even though the overall effect of cell–cell interactions on the spreading of cells may be indistinguishable from that of Brownian motion.

The effect of volume fraction on the normalized angular probability density defined by (4.1) has been investigated, and the results are shown in figure 16(*a*) ($G_{bh} = 10$ and $\beta = 5$). We see that $p'(\theta)$ has a larger peak at $\theta = 0$ for smaller values of c. If there is no interaction between squirmers, every bottom-heavy squirmer has its orientation in the y-direction, and the $p'(\theta)$ distribution becomes the Dirac delta function (Brenner & Weissman 1972). The spread in the orientation is caused by the interaction, and the interaction increases with increasing c. An effective value of λ in the function given by (4.3) is obtained from a least-squares fit ($\lambda = 13.3, 2.43$ for $c = 0.025, 0.1$, respectively), and the comparisons with the numerical results are shown in figure 16(*b*). We see that the results for $c = 0.025$ do not correspond well with the equation (4.3), though the results for $c = 0.1$ show good agreement, as seen in figure 12.

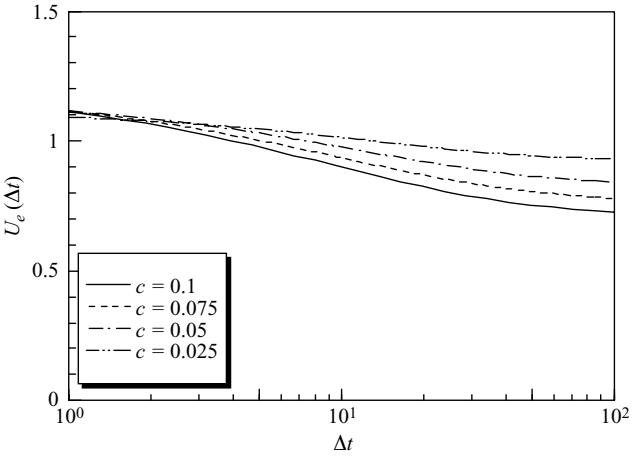

FIGURE 17. Effect of c on the effective velocity of bottom-heavy squirmers ($G_{bh} = 10$ and $\beta = 5$). (*a*) Translational diffusivity D^T_{xx}, (*b*) rotational diffusivity D^R_{yy}.

The effect of volume fraction on the effective velocity is shown in figure 17 ($G_{bh} = 10$ and $\beta = 5$). We see that the effective velocity decreases with increasing c at large Δt. This is again because the interaction between squirmers increases with c, and the interaction prevents them from swimming in straight lines. The constant upward velocity also decreases with increasing c. The absolute value of the instantaneous velocity, $U_e(0)$, slightly increases with c, though this is barely distinguishable in figure 17. The hydrodynamic interaction has the effect of increasing the velocity in the semi-dilute regime, as mentioned before. The effect of volume fraction on the translational and rotational diffusivities is also investigated, and the results show that the diffusivity (when it exists) increases as c increases. The results are straightforward, so they are omitted in this paper.

In figure 9(*a*), the translational diffusivity of non-bottom-heavy squirmers was shown to be dominated by the mean free path. We have constructed an analogous diagram from the results for $G_{bh} = 10$ and $\beta = 5$, sorted by $\Delta t/t_{mfp}$, but the curves do not overlap well and are not presented. In the case of bottom-heavy squirmers, most of them swim in more-or-less the same direction, and they experience fewer near-collisions than non-bottom-heavy squirmers with isotropic orientations. Therefore, the mean free path is not a dominant length scale for the translational diffusivity, and the interaction between squirmers is more likely to be dominated by the configuration of surrounding squirmers. The length scale over which the configuration changes is approximately that of the mean particle spacing, ℓ_{mps}, which is given by

$$\ell_{mps} = \left(\frac{4\pi a^3}{3c}\right)^{1/3}; \tag{4.5}$$

this corresponds to a time-scale for configuration changes of $t_{mps} = \ell_{mps}/U_{sol}$. In dimensionless terms this is

$$t_{mps} = (4\pi/3c)^{1/3}. \tag{4.6}$$

So the results for the translational diffusivity have been plotted in terms of $\Delta t/t_{mps}$ and are shown in figure 18(*a*). We see that all the curves overlap well and change their inclination around $\Delta t/t_{mps} \approx 7$. When most of the squirmers swim in a similar

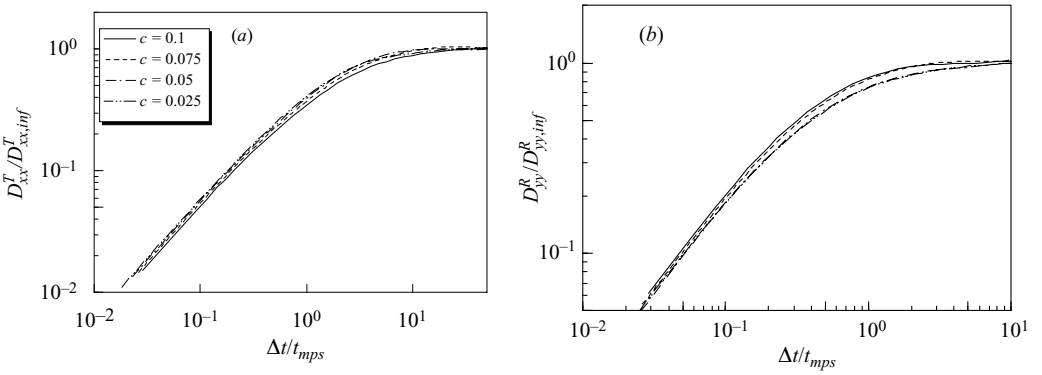

FIGURE 18. The diffusivities are plotted in terms of $\Delta t/t_{mps}$. The vertical axis is normalized by D_{inf}.

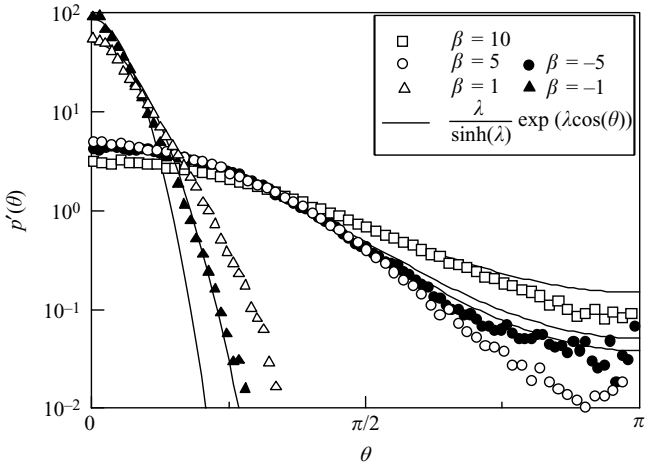

FIGURE 19. Effect of β on the normalized probability density function distribution ($G_{bh} = 10$ and $c = 0.1$). The function is fitted by the method of least squares.

direction, the configuration of squirmers does not change significantly over a time interval of $\Delta t/t_{mps} = 1$, so the characteristic length scale in this case is much longer than l_{mps}.

The rotational diffusivity is plotted in terms of $\Delta t/t_{mps}$, and the results for D^R_{yy} are shown in figure 18(*b*). We see again that all the curves overlap well and change their inclination around $t_{mps} \approx 1$. We also constructed an analogous diagram sorted by unscaled Δt instead of t_{mps}, but the curves do not overlap well and are not presented. We can say, therefore, that the rotational diffusivity of bottom-heavy squirmers is strongly influenced by the mean particle separation.

The results for the normalized angular probability density with $|\beta| = 1$, 5 and 10 are shown in figure 19 ($G_{bh} = 10$ and $c = 0.1$). An effective value of λ in the function given by (4.3) is obtained from a least-squares fit ($\lambda = 2.24, 43.5, 25.3, 2.43, 1.54$ for $\beta = -5, -1, 1, 5, 10$, respectively), and the curves are shown in the figure as well. We see that $p'(\theta)$ has a larger peak at $\theta = 0$ for smaller $|\beta|$. The spread in the orientation is caused by the interactions between squirmers, and the interactions increase with

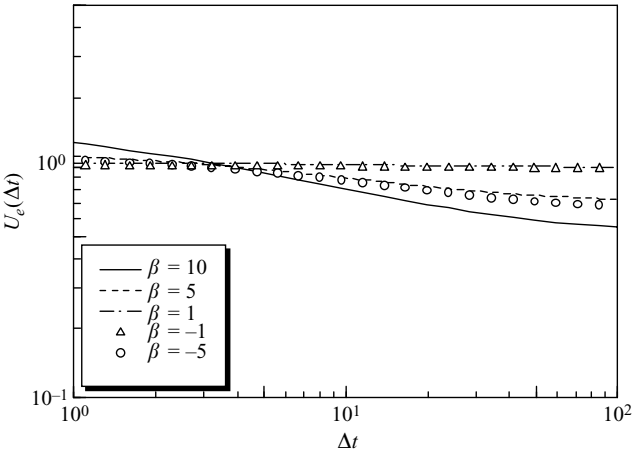

FIGURE 20. Effect of β on the effective velocity of bottom-heavy squirmers ($G_{bh} = 10$ and $c = 0.1$).

increasing $|\beta|$. The results show better agreement with equation (4.3) at larger $|\beta|$, when the hydrodynamic interactions are stronger; in this sense the effect of $|\beta|$ is similar to that of c.

The effect of β on the effective velocity is shown in figure 20 ($G_{bh} = 10$ and $c = 0.1$). We see again that the effective velocity decreases with increasing $|\beta|$ when $\Delta t > 10$. This is because the interaction between squirmers increases with $|\beta|$, and the interaction prevents them from swimming upwards in straight lines. The sign of β does not greatly influence these results. The absolute value of the instantaneous velocity, $U_e(0)$, again increases in large $|\beta|$ cases, because the far-field hydrodynamic interaction tends to increase the velocity in the semi-dilute regime, as mentioned before. The effect of β on the translational and rotational diffusivities is also investigated, and the results show that the diffusivity (when it exists) increases as $|\beta|$ increases. The results are again straightforward, so they are omitted.

5. Summary and discussion

In the case of *non-bottom-heavy* squirmers, the translational and rotational spreading of squirmers are correctly described as diffusive processes over a sufficiently long time scale, even though all the movements of individual squirmers are deterministically calculated. The translational diffusivity decreases with increasing c and β, and the rotational diffusivity increases with increasing c and β. The effective velocity decreases more rapidly with time as c and β are increased, and the absolute value of the instantaneous velocity, $U_e(0)$, increases with c and β in the semi-dilute regime.

Hill & Häder (1997) measured the rotational diffusivity of *C. nivalis* in a dilute suspension with no imposed background flow, and the result for the dimensionless rotational diffusivity D^R was roughly in the range 0.03–0.17. Vladimirov *et al.* (2000, 2004) used a more sophisticated method to measure the rotational diffusivity of *C. nivalis*, and obtained the dimensionless results of $D^R = 1 \times 10^{-3}$–6×10^{-3}. These experiments used dilute suspensions, so the mechanism of the diffusive process is not hydrodynamic interaction but the intrinsic randomness of individual cells. The rotational diffusivity obtained in this study (in the parameter range of $c = 0.025 - 0.1$

and $\beta = 1 - 10$) gives D^R in the range 0.09–0.2, which is larger than the values measured by Vladimirov *et al.* Therefore, the hydrodynamic interaction between cells at such volume fractions is at least as important as their intrinsic randomness in determining their diffusive behaviour, and is likely to be a major factor in the diffusivity of micro-organisms in a semi-dilute suspension (and even more so in a concentrated suspension).

If the characteristic time scale of the phenomena of interest is longer than the time scale for squirmers to show diffusivity, one can use a continuum model for those phenomena, in which the translational and rotational spreading of squirmers are described by means of diffusion tensors. This treatment sounds similar to that for Brownian particles; however, there are some essential differences. First of all, there is a finite Brownian diffusivity even for a single particle, i.e. $c \to 0$, while the diffusivity of squirmers varies as c^{-1} (translational – (3.7)) or c (rotational – (3.8)). This is because Brownian motion is induced by the interaction between a particle and molecules of the solvent fluid, but the diffusion of squirmers is induced only by the interaction between particles. Since the sizes of the interacting particles are very different, the time scale to show diffusivity is also different. If one assumes that the micro-organisms swim in water at 10 body lengths per second, dimensional $t_{mfp}(=4a/(3cU_{sol}))$ is 0.66 s for $c = 0.1$ and 6.6 s for $c = 0.01$, and dimensional $t_{mps}(=[\sqrt{4\pi a^3/(3c)}]^{-3}/U_{sol})$ is 0.17 s for $c = 0.1$ and 0.37 s for $c = 0.01$. The characteristic time scale for Brownian motion is much shorter than this. In the case of Brownian particles, the translational and rotational diffusivities are given by (1.3). Both of them increase with the temperature, and the dimensionless D^R is equal to three-quarters of dimensionless D^T. In the case of squirmers, however, D^R is much less than D^T, and the changes of D^T and D^R with c and β are in the opposite sense.

In the case of *bottom-heavy* squirmers, the normalized probability density shows good agreement with equation (4.3) when the effect of hydrodynamic interaction is more important than the bottom-heaviness. In such cases, the rotational spreading of squirmers can be modelled as a biased random walk after a sufficiently long time. The translational spreading of bottom-heavy squirmers in the horizontal direction can also be correctly described as a diffusive process over a sufficiently long time scale, and the same is true for the vertical spreading relative to the average upward velocity. Both translational and rotational diffusivities are increasingly suppressed with increasing G_{bh}. The effects of c and β do not change the results qualitatively, and the diffusivities increase with increasing c and β.

The rotational diffusivities of bottom-heavy squirmers obtained in this study (in the parameter range of $G_{bh} = 10$–100, $c = 0.025$–0.1 and $\beta = 1$–10) are in the range of $D^R_{xx} = 0.001$–0.18 and $D^R_{yy} = 0.005$–0.23, which are comparable or larger than the results of Vladimirov *et al.* ($D^R = 1 \times 10^{-3}$–6×10^{-3}). We have, therefore, concluded that the hydrodynamic interaction between cells can be a major factor in determining the diffusivity of bottom-heavy micro-organisms in a semi-dilute suspension. Figure 21 shows the correlations between the xx- and yy-components of D^R_{inf} and c, in which a linear function is fitted by the method of least squares. It is found that both components of the rotational diffusivity of bottom-heavy squirmers are roughly proportional to c, similar to the results for non-bottom-heavy squirmers.

T. I. was supported by a JSPS postdoctoral fellowship for research abroad from 2003 to 2005. We are very grateful to J. T. Locsei for his contribution to the scaling arguments of § 3.2.

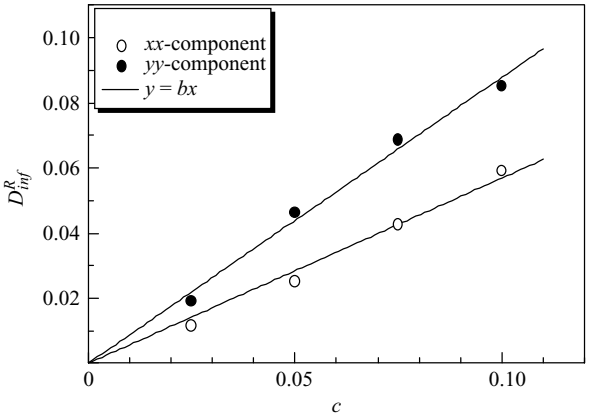

FIGURE 21. Correlation between D^R_{inf} and c ($G_{bh} = 10$, $\beta = 5$). D^R_{inf} is the converged rotational diffusivity after a sufficiently long time.

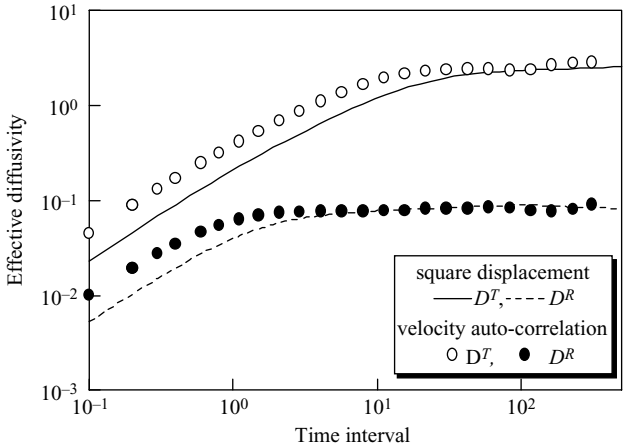

FIGURE 22. Comparison of D^T and D^R calculated from the square displacement and the velocity auto-correlation for non-bottom-heavy squirmers with $\beta = 5$.

Appendix. Comparison of diffusivities calculated from the square displacement and the velocity auto-correlation

The aim of this appendix is to compare the translational and rotational diffusivities calculated from the square displacement and the velocity auto-correlation. The diffusivities were defined by equations (2.5) and (2.6). If the time interval is long enough, diffusivities calculated both by the square displacement and the velocity auto-correlation should be the same. When the time interval is shorter, however, the diffusivity calculated by the velocity auto-correlation should be twice as large as that calculated by the square displacement. This can be shown by substituting into (2.5) the Taylor series for $\langle \boldsymbol{U}(t)\boldsymbol{U}(0)\rangle$ as

$$\langle [\boldsymbol{r}(t) - \boldsymbol{r}(0)]^2 \rangle = t^2 \langle \boldsymbol{U}(0)^2 \rangle + \cdots. \tag{A 1}$$

In figure 22, we plot the diffusivities, for non-bottom-heavy squirmers with $\beta = 5$, calculated from the square displacement and the velocity auto-correlation. We see

that the diffusivity calculated by the velocity auto-correlation is twice as large as that calculated by the square displacement for short enough time intervals, as predicted. Moreover, the two diffusivities coincide for long enough time intervals, from which we can confirm the reliability of the present results. We also calculated the two diffusivities in other cases used in this study, and they again coincide for long enough time intervals.

REFERENCES

Acrivos, A. 1995 Bingham award lecture 1994: Shear-induced particle diffusion in concentrated suspensions of noncolloidal particles. *J. Rheol.* **39**, 813–826.

Batchelor, G. K. & Green, J. T. 1972*b* The determination of the bulk stress in a suspension of spherical particles to order c^2. *J. Fluid Mech.* **56**, 401–427.

Batchelor, G. K. 1976 Brownian diffusion of particles with hydrodynamic interaction. *J. Fluid Mech.* **75**, 1–29.

Bees, M. A. & Hill N. A. 1998 Linear bioconvection in a suspension of randomly-swimming, gyrotactic micro-organisms. *Phys. Fluids* **10**, 1864–1881.

Blake, J. R. 1971 A spherical envelope approach to ciliary propulsion. *J. Fluid Mech.* **46**, 199–208.

Bossis, G. & Brady, J. F. 1984 Dynamic simulation of sheared suspensions. Part I. General method. *J. Chem. Phys.* **80**, 5141–5154.

Brady, J. F. & Bossis, G. 1985 The rheology of concentrated suspensions of spheres in simple shear flow by numerical simulation. *J. Fluid Mech.* **155**, 105–129.

Brady, J. F. & Bossis, G. 1988 Stokesian dynamics. *Annu. Rev. Fluid Mech.* **20**, 111–157.

Breedveld, V., Ende, D. V. D., Tripathi, A. & Acrivos, A. 1998 The measurement of the shear-induced particle and fluid tracer diffusivities in concentrated suspensions by a novel method. *J. Fluid Mech.* **375**, 297–318.

Brennen, C. & Winet, H. 1977 Fluid mechanics of propulsion by cilia and flagella. *Annu. Rev. Fluid Mech.* **9**, 339–398.

Brenner, H. & Weissman, M. H. 1972 Rheology of a dilute suspension of dipolar spherical particles in an external field. Part II. Effects of Rotary Brownian motion. *J. Colloid Interface Sci.* **41**, 499–531.

Childress, S., Levandowsky, M. & Spiegel, E. A. 1975 Pattern formation in a suspension of swimming micro-organisms: Equations and stability theory. *J. Fluid Mech.* **63**, 591–613.

Dratler, D. I. & Schowalter, W. R. 1996 Dynamic simulation of suspensions of non-Brownian hard spheres. *J. Fluid Mech.* **325**, 53–77.

Drazer, G., Koplik, J., Khusid, B. & Acrivos, A. 2002 Deterministic and stochastic behaviour of non-Brownian spheres in sheared suspensions. *J. Fluid Mech.* **460**, 307–335.

Foss, D. & Brady, J. F. 1999 Self-diffusion in sheared suspensions by dynamic simulation. *J. Fluid Mech.* **401**, 243–274.

Foss, D. & Brady, J. F. 2000 Structure, diffusion and rheology of Brownian suspensions by Stokesian dynamics simulation. *J. Fluid Mech.* **407**, 167–200.

Hill, N. A. & Häder, D.-P. 1997 A biased random walk model for the trajectories of swimming micro-organisms. *J. Theor. Biol.* **186**, 503–526.

Hillesdon, A. J., Pedley, T. J. & Kessler, J. O. 1995 The development of concentration gradients in a suspension of chemotactic bacteria. *Bull. Math. Biol.* **57**, 299–344.

Ishikawa, T. & Pedley, T. J. 2007 The rheology of a semi-dilute suspension of swimming model micro-organisms. *J. Fluid Mech.* **588**, 399–435.

Ishikawa, T., Simmonds, M. P. & Pedley, T. J. 2006 Hydrodynamic interaction of two swimming model micro-organisms. *J. Fluid Mech.* **568**, 119–160.

Kessler, J. O. 1985*a* Hydrodynamic focusing of motile algal cells. *Nature* **313**, 218–220.

Kessler, J. O. 1985*b* Co-operative and concentrative phenomena of swimming micro-organisms. *Contemp. Phys.* **26**, 147–166.

Kessler, J. O. 1986*a* The external dynamics of swimming micro-organisms. In *Progress in Phycological Research*, vol. 4 (ed. F. E. Round & D. J. Chapman), pp. 257–307. Biopress.

Kessler, J. O. 1986*b* Individual and collective dynamics of swimming cells. *J. Fluid Mech.* **173**, 191–205.

Kessler, J. O., Hill, N. A. & Häder, D.-P. 1992 Orientation of swimming flagellates by simultaneously acting external factors. *J. Phycology* **28**, 816–822.

Kim, S. & Karrila, S. J. 1992 *Microhydrodynamics: Principles and Selected Applications.* Butterworth–Heinemann.

Lighthill, M. J. 1952 On the squirming motion of nearly spherical deformable bodies through liquids at very small Reynolds numbers. *Commun. Pure Appl. Maths.* **5**, 109–118.

Magar, V., Goto, T. & Pedley, T. J. 2003 Nutrient uptake by a self-propelled steady squirmer. *Q. J. Mech. Appl. Maths* **56**, 65–91.

Marchiro, M. & Acrivos, A. 2001 Shear-induced particle diffusivities from numerical simulations. *J. Fluid Mech.* **443**, 101–128.

Metcalfe, A. M. & Pedley, T. J. 2001 Falling plumes in bacterial bioconvection. *J. Fluid Mech.* **445**, 121–149.

Metcalfe, A. M., Pedley, T. J. & Thingstad, T. F. 2004 Incorporating turbulence into a plankton foodweb model. *J. Marine Systems* **49**, 105–122.

O'Brien, R. W. 1979 A method for the calculation of the effective transport properties of suspensions of interacting particles. *J. Fluid Mech.* **91**, 17–39.

Pedley, T. J. & Kessler, J. O. 1987 The orientation of spheroidal microorganisms swimming in a flow field. *Proc. R. Soc. Lond.* B **231**, 47–70.

Pedley, T. J. & Kessler, J. O. 1990 A new continuum model for suspensions of gyrotactic micro-organisms. *J. Fluid Mech.* **212**, 155–182.

Pedley, T. J. & Kessler, J. O. 1992 Hydrodynamic phenomena in suspensions of swimming microorganisms. *Annu. Rev. Fluid Mech.* **24**, 313–358.

Sierou, A. & Brady, J. F. 2004 Shear-induced self-diffusion in non-colloidal suspensions. *J. Fluid Mech.* **506**, 285–314.

Vladimirov, V. A., Denissenko, P. V., Pedley, T. J., Wu, M. & Moskalev, I. S. 2000 Algal motility measured by a laser-based tracking method. *Mar. Freshwater Res.* **51**, 589–600.

Vladimirov, V. A., Wu, M. S. C., Pedley, T. J., Denissenko, P. V. & Zakhidova, S. G. 2004 Measurement of cell velocity distributions in populations of motile algae. *J. Expl Biol.* **207**, 1203–1216.

Wang, Y., Murai, R. & Acrivos, A. 1998 Transverse shear-induced gradient diffusion in a dilute suspension of spheres. *J. Fluid Mech.* **357**, 279–287.